

Noninjection Facile Synthesis of Gram-Scale Highly Luminescent CdSe Multipod Nanocrystals

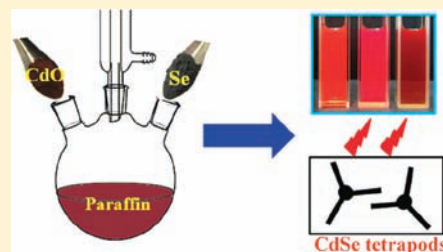
Wenjin Zhang,[†] Chan Jin,[‡] Yongji Yang,[‡] and Xinhua Zhong^{*,†}

[†]Shanghai Key Laboratory of Functional Materials Chemistry, Department of Chemistry, East China University of Science and Technology, Shanghai, 200237, China

[‡]Department of Biophysics, Second Military Medical University, Shanghai 200433, China

S Supporting Information

ABSTRACT: Nearly all reported approaches for synthesis of high quality CdSe nanocrystals (NCs) involved two steps of preparation of Cd or Se stock solution in advance and then mixing the two reactants via hot-injection in high temperature. In this manuscript, Gram-scale CdSe multipod NCs were facily synthesized in a noninjection route with the use of CdO and Se powder directly as reactants in paraffin reaction medium containing small amount of oleic acid and trioctylphosphine. The influence of various experimental variables, including reaction temperature, nature and amount of surfactants, Cd-to-Se ratio, and the nature of reactants, on the morphology of the obtained CdSe NCs have been systematically investigated. After deposition of ZnS shell around the CdSe multipod NCs, the PL QY of the obtained CdSe/ZnS can be up to 85%. The reported noninjection preparation approach can satisfy the requirement of industrial production bearing the advantage of low-cost, reproducible, and scalable. Furthermore, this facile noninjection strategy provides a versatile route to large-scale preparation of other semiconductor NCs with multipod or other morphologies.



INTRODUCTION

Control over the size and morphology is of great importance for tailoring electronic structure and excitons dynamics in semiconductor nanocrystals (NCs).¹ Morphology control, especially in industrial scale, represents the next stage in NCs synthesis. Branched topologies of NCs, especially the multipodal (including tripodal and tetrapodal) shape, can potentially lead to a variety of interesting mechanical, optical/electric, and chemical properties different from those of spherical nanoparticles, and thus be useful in the reinforcement of polymers, assembly of materials, and fabrication of photovoltaic devices.^{2–4} Up to date, tetrapod-shaped NCs have been synthesized for a variety of single component II–VI, IV–VI semiconductors such as ZnO,⁵ ZnSe,⁶ CdS,⁷ CdTe,^{2a,8} CdSe,^{8c,9} PbS,¹⁰ and PbSe¹¹ by delicately balancing the reaction parameters to achieve separate nucleation and growth stages in one reaction, in which the growth of tetrapod NCs started with zinc blende nuclei and grew arms in a wurtzite manner. Recently, a seeded growth technique of preparing tetrapod NCs was proposed to conduct the growth of zinc blende core and wurtzite branched shell in two independent reactions, and accordingly multicomponent core/shell tetrapods of CdSe, CdTe, or ZnTe cores with CdX (X = Se, S, Te) arms were constructed.^{12–14} However, the previously commonly adopted hot-injection method, in which a precursor solution is rapidly introduced into heated organic solvent, is difficult to scale up such a synthesis for making NCs in large quantities. Therefore, with the growing interest in applications based on multipod NCs comes a need and remains a great challenge to develop a

scalable, reproducible, environmentally friendly, and low cost preparation route aimed at producing high quality nanomaterials for potential industrial applications.

CdSe is one of the most popular semiconductor materials in the chemical synthesis of NCs, but growing homogeneous samples of CdSe multipods in a controlled fashion was difficult, and an efficient low-cost and scaled up route for the preparation of CdSe multipod NC is missing. It is noted that most approaches for the synthesis of high quality (good size and shape monodispersity, good optical performance) CdSe NCs,¹⁵ in which CdSe multipods are included,⁹ involved the injection of precursor at high temperature with the use of large amount of expensive alkylphosphonates, trioctylphosphine oxide and/or alkylamines as surfactants or reaction solvent, and thus Cd or Se precursor stock solution should be prepared separately in advance. These synthetic approaches cannot satisfy the low-cost, reproducible and scalable requirement for industrial production.

Herein, for the first time we reported a facile noninjection, gram-scale synthesis of CdSe multipods in high yield with use of CdO and Se powder directly as reactants in paraffin media. All reactants are commercial available and no precursor stock solutions were prepared in advance. Accordingly our reported preparation approach can satisfy the requirement of industrial production bearing the advantage of low-cost, reproducible, and scalable. In addition, after deposition of ZnS around the CdSe

Received: September 10, 2011

Published: December 13, 2011

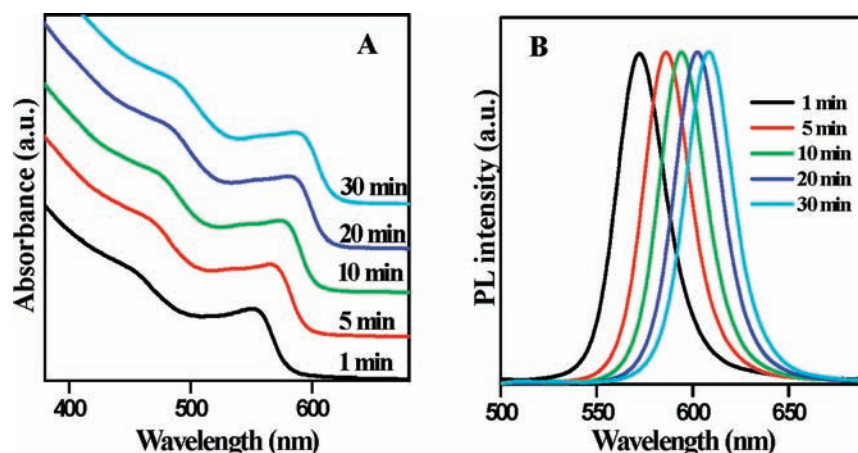


Figure 1. Temporal evolution of UV–vis absorption (A) and PL emission ($\lambda_{\text{ex}} = 350$ nm, B) spectra of CdSe NCs growth at 210 °C.

multipod NCs, the photoluminescence quantum yield (PL QY) of the obtained CdSe/ZnS can be up to 85%. Furthermore, this facile noninjection strategy provides a versatile route to large-scale preparation of other semiconductor NCs with multipod or other morphologies.

EXPERIMENTAL SECTION

Gram-Scale Synthesis of Multipodal CdSe NCs. In a typical synthesis, CdO (1.15 g, 9 mmol) and Se (100 mesh, 0.47 g, 6 mmol) were mixed with 10.0 mL of trioctylphosphine, 15.0 mL of oleic acid, and 150 mL of paraffin in a 500 mL three-necked flask. The mixture was then degassed at room temperature for 5 min. After that, the solution was heated to 210 °C at a heating rate of 20 °C/min under N_2 flow. During the reaction, aliquots were taken with a syringe at different times to monitor the growth of CdSe NCs by recording UV–vis absorption and PL emission spectra. Afterward, the reaction solution was cooled to ~ 80 °C and precipitated by acetone. The flocculent precipitate that formed was centrifuged, while the supernatant liquid was decanted, and the isolated solid was dispersed in toluene or chloroform. The above centrifugation and isolation procedure was then repeated several times for purification of the prepared CdSe NCs. Finally, the products were redispersed in toluene or chloroform or dried under vacuum for further analyses. Product yield was 90% based on Se (1.01 g of CdSe NCs).

Overcoating ZnS Shell around CdSe Multipod NCs. In this experiment, CdSe core NCs were synthesized under the reaction of 0.15 mmol of CdO, 0.1 mmol of Se powder in 4.0 mL of paraffin containing 0.2 mL of TOP, and 0.3 mL of oleic acid. Other procedure and operation were identical to those of gram-scale synthesis described above. When CdSe NCs growth at 210 °C for 2 min, reaction temperature was lowered down to 140 °C, then 0.3 mL of 0.1 M zinc dimethyldithiocarbamate (ZDC) stock solution (prepared by the dissolution of ZDC in 1:1 oleyl amine/paraffin at room temperature), and 0.3 mL of 0.4 M $\text{Zn}(\text{OAc})_2$ solution (obtained by dissolution of 8 mmol of $\text{Zn}(\text{OAc})_2$ in 6.0 mL oleyl amine and 14 mL paraffin at 120 °C) were added into the reaction system, followed by the addition of 0.5 mL oleyl amine. Reaction temperature was kept at 140 °C for another 30 min. After that, reaction temperature was raised to 200 °C and kept for 20 min. When the optical spectra showed no further changes, the second batch of ZnS shell was deposited with the use of equal amount of precursors following the same heating procedure. After finishing shell deposition, the purification of the obtained core/shell NCs was similar to that of plain CdSe core NCs.

Characterization. UV–vis and PL spectra were obtained on a Shimadzu UV-2450 UV–vis spectrophotometer and a Cary Eclipse (Varian) fluorescence spectrophotometer, respectively. The room-temperature PL QY was determined by comparing the integrated emission of the QDs samples in chloroform with that of a fluorescent dye (such as rhodamine 6 G with QY of 95% or rhodamine 640 with

QY of 100%) in ethanol with identical optical density.¹⁶ A quadratic refractive index correction was done in order to compensate the different refractive index of the different solvents used for organic dyes and QDs. Also the known QYs of the QDs in solution can be used to measure the PL efficiencies of other QDs by comparing their integrated emission. To conduct investigations in the transmission electron microscopy (TEM), the NCs were deposited from dilute toluene solutions onto copper grids with carbon support by slowly evaporating the solvent in air at room temperature. TEM and high resolution (HR) TEM images were acquired using a JEOL JEM-2010 transmission electron microscope operating at an acceleration voltage of 200 kV. Powder X-ray diffraction (XRD) was obtained by wide-angle X-ray scattering, using a Siemens D5005 X-ray powder diffractometer equipped with graphite monochromatized $\text{Cu K}\alpha$ radiation ($\lambda = 1.54178$ Å). XRD samples were prepared by depositing NC powder on a piece of Si (100) wafer.

RESULTS AND DISCUSSION

The CdSe multipod NCs were prepared with the use of CdO and Se powder as reactant in paraffin media containing small amount of oleic acid and trioctylphosphine (TOP) at temperature of 190–250 °C. The proceeding of the reaction is ascribed to the in situ formation of cadmium oleate and TOP-Se at high temperature due to the presence of excess amount of oleic acid and TOP in relative to CdO and Se powder. In a typical synthesis, CdO and selenium powder were loaded in a mixture solvent containing trioctylphosphine, oleic acid, and paraffin at room temperature. With increase of reaction temperature to 160 °C, CdO and Se dissolved gradually, and the initially turbid reaction system turned to clear gradually and CdSe NCs were formed accordingly. This was indicated by the appearance of light-red color of the reaction media. As the CdSe NCs grew, the dissolution of CdO and Se was accelerated and the newly formed monomer added to CdSe nuclei and brought forward the increase of particle size quickly. The reaction at 210 °C can be nearly finished in a period of 10 min, which was indicated by no variation in the optical spectra.

Figure 1 shows the temporal evolution of UV–vis absorption and PL emission spectra of the as-prepared CdSe NCs. Both the sharp first excitonic absorption peak in the UV spectra and the narrow and symmetric emission peak in the PL spectra indicate the fact that particle size and shape are nearly monodispersed. Furthermore, from the optical spectra we can find that the peak shape in both UV and PL spectra remained unchanged and the PL peak width kept at a narrow value. After 30 min growth/annealing, the PL peak position can approach

from 573 to 607 nm with a narrow peak width of fwhm (full width at half-maximum) in the range of 24–27 nm. The PL QY of the obtained CdSe multipods was less than 3%, which is similar to previous cases,⁹ and the weak PL was quenched nearly completely after 1 h annealing.

The morphology and size of the typical CdSe Ns from this synthesis are shown in Figure 2. Interestingly, the obtained

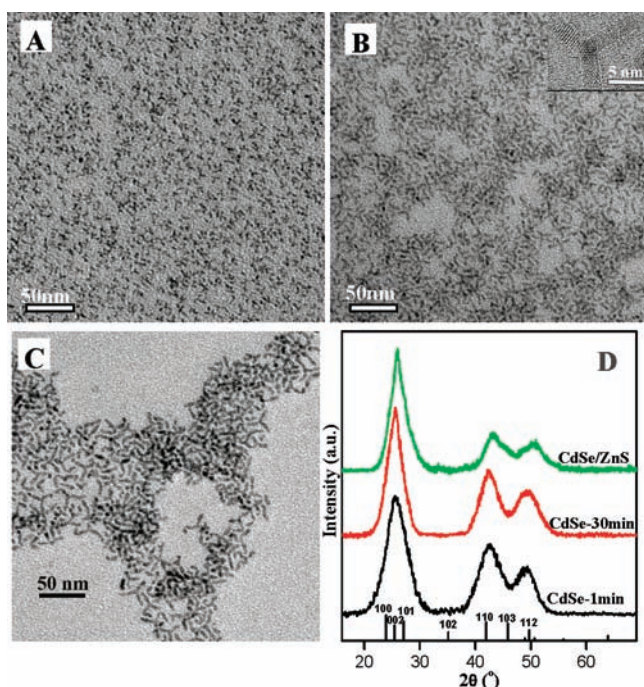


Figure 2. Wide-field TEM images of CdSe multipod NCs growth at 210 °C for 2 min (A) and 30 min (B), and corresponding CdSe/ZnS core/shell NCs starting from CdSe core with growth time of 2 min (C). HRTEM image of a typical tetrapod. (D) XRD patterns of CdSe multipods and corresponding CdSe/ZnS core/shell NCs.

CdSe NCs were unexpectedly found to be tripod- or tetrapod-shape. Because of the small size, it is difficult to distinguish between tripod and tetrapod. Accordingly we classified the tripod and tetrapod as multipod. In our statistic of over 200 nanostructures, multipods accounted for 92%, and the balance comprised bipods, and irregular shapes. No spherical particles were observed. The average arm length/width for samples with growth time of 2 and 30 min were $6.7 \pm 1.0/2.1 \pm 0.3$, and $12.2 \pm 1.5/3.4 \pm 0.4$ nm, respectively. It was found that the aspect ratio of arms in multipods kept at a relatively constant value under different growth times. Without having to perform post preparative size sorting, we found that the obtained gram-scaled CdSe multipods were also of higher quality (i.e., higher selectivity toward the multipod shape and more uniform dimensions) than most of previous reported literature.⁹ Inset of Figure 2B shows a typical HRTEM image of a single CdSe tetrapod formed by a core and four arms, which are viewed along the CdSe core direction. Therefore, the central CdSe arm fully overlaps with the core, while the other three arms are equally oriented with respect to the substrate. The HRTEM image shows that the arms in a tetrapod are structurally uniform, and the well-defined one-dimensional lattice fringes go straight through the whole structure without stacking faults or twins. The arms in a tetrapod are rice-shaped and nearly equal in length and diameter. To determine the crystal phase of arms

in tetrapods, we selected a tetrapod displaying two-dimensional lattice fringes (Figure S1 in Supporting Information, SI). The analysis of the reciprocal lattice peaks obtained from a 2D fast Fourier transform (FFT) of the HRTEM images (inset of Supporting Information Figure S1) confirms wurtzite lattice for the arm. Even though the XRD patterns of the obtained CdSe NCs (Figure 2D) look more like a zinc blende structure, the typical (400) peak at 61.0° corresponding to zinc blende structure is not observed. Because of the small particle size, the XRD pattern cannot give an unambiguous evidence to determine the crystal phase. In fact with the increase of particle size, the characteristic (100) and (101) peaks of wurtzite phase appear on the shoulder side of the (002) peak as indicated in the XRD pattern of CdSe/ZnS sample. The observed wurtzite phase in the arms of tetrapods is expected since the most credited and simplest explanation for the formation of tetrapod-shaped NCs in II–VI group semiconductor, including CdSe, is that they nucleate in the cubic phase and grow in wurtzite arms.^{2a}

Similar to previous cases,⁹ the PL QY of our obtained CdSe multipods is quite low (<3%). To improve the emission efficiency, the common route of depositing a higher band gap material ZnS around the CdSe core template was adopted. A modified shell deposition technique was adopted for the overgrowth of ZnS shell by the thermal decomposition of single molecular precursor zinc dimethyldithiocarbamate (ZDC) in the CdSe multipod NCs crude reaction solution.¹⁷ In the thermal decomposition of ZDC, equimolar amount of zinc stearate was added together with ZDC to compensate the missing quantity of zinc precursor in ZDC (the Zn/S ratio in ZDC is 1:4). The overcoated ZnS layer serves as a type-I heterojunction with the CdSe (e.g., the conduction of the shell material is higher than that of core material while the valence band of the shell material is lower than that of the core material), thus efficiently confining excitons within the CdSe core region and substantially enhancing the spatial direct radiative recombination at the CdSe. Therefore, depositing ZnS shell can remarkably improve PL QY and stability of the obtained heterostructures.

Experimental results showed that with the deposition of ZnS, both the first excitonic absorption peak in the absorption spectrum and PL peak in the PL emission spectrum red-shifted substantially accompanied with enhanced PL emission efficiency (Figure 3). With the thermal decomposition of ZDC and the formation of ZnS shell around CdSe template, the PL emission wavelength can shift from the initial 585 to 630 nm, the highest PL QY can be up to 85%, and the fwhm of PL peak was preserved as narrow as 23–25 nm. Such narrow PL peak width and high QY is among the best values in the tetrapod-shaped NCs and also a superior value for the spherical NCs.^{9,15} The bright luminescence of the obtained CdSe/ZnS heterostructures can be observed even in room light (Figure 3C). It should be noted that multipod NCs with high PL QYs is not commonly observed and the reported highest PL QY of 50% is found in CdSe/CdS tetrapods and 60% for CdSe/ZnS tetrapods in refs 13a and 14, respectively. The substantial red-shift in the process of ZnS deposition is not solely due to the formation of ZnS layer, the contribution from the further growth of CdSe, and the formation of CdS constituent cannot be excluded. The formation of CdS constituent is stemmed from the excess stoichiometric amount of Cd precursor used in the synthesis of CdSe and the support of sulfur source in the thermal decomposition of ZDC. Because of the narrower band

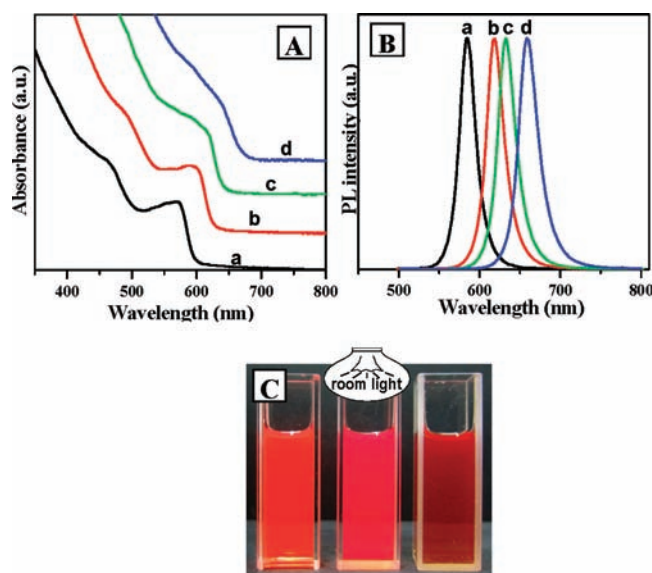


Figure 3. Normalized UV-vis absorption spectra (A) and PL emission spectra (B, $\lambda_{\text{exc}} = 360$ nm) of CdSe multipod NCs based core/shell structure with different ZnS shell thickness (a: plain CdSe multipods with growth time of 2 min; b, c: 1- and 2-cycle deposition of ZnS, respectively; d: 1 cycle of CdS + 2 cycles of ZnS). (C) Photograph of the typical emission colors of the obtained CdSe/ZnS core/shell multipod NCs under room-light radiation.

gap of CdS ($E_g = 2.45$ eV) in compared with that of ZnS ($E_g = 3.67$ eV), the deposition of CdS shell can bring forward a greater red-shift of the emission wavelength than that from ZnS shell. Previous samples of CdSe/CdS, CdSe/CdS/ZnS has proven this assumption.¹⁸ Based on this fact, in order to obtain longer emission wavelength, CdS shell was intentionally deposited first with the thermally decomposition of single molecular precursor cadmium dimethyldithiocarbamate (CDC) followed by the deposition of ZnS shell. Following this procedure, the PL emission wavelength could be further tuned to 664 nm (curve d in Figure 3B). Furthermore, when larger CdSe core materials were used (i.e., the starting CdSe core NCs were prepared at higher reaction temperature such as 230 or 250 °C), longer emission wavelength can be obtained in the core/shell nanostructures. After the deposition of ZnS, the original multipod morphology was still conserved. The corresponding TEM images of the obtained CdSe/ZnS are shown in Figure 2C.

A series of experimental variables, including growth temperature, nature and amount of surfactants, Cd/Se ratio, and the nature of reactants, were systematically investigated to study their influence on this particular morphology (detailed experimental procedure and results were given in Supporting Information). It was found that higher growth temperature (such as 230, 250 °C) favored for formation of multipods with larger-sized diameter of arms. Higher temperature brings forward higher concentration of monomer, which promotes the relative faster growth of radial direction of rods. Besides oleic acid, stearic acid and dodecanoic acid (DDA) were also used in replacement of oleic acid. Experimental results showed that in the case of DDA, longest arm length can be obtained and accordingly the aspect ratio of the obtained multipods is larger than the other two cases. There was no substantial difference in the resulting morphology of the obtained NCs between the cases of oleic acid and steric acid. Experimental

results demonstrated that the presence of TOP is crucial for the formation of multipod morphology. When no TOP was used in the reaction media, small sized (~ 3 nm) dots or irregular dots were obtained and the percentage of tripod- or tetrapod-shaped NCs was negligible. When the amount of TOP was increased to 0.5 mL, the obtained multipods have shorter arm length. There was no substantial variation in the morphology when paraffin was replaced by another common noncoordinating solvent 1-octadecene (ODE). The Cd/Se ratios of 1.5:1, 1:1, and 1:1.5 were tested. Experimental results demonstrated that excessive amount of Cd precursor favored for the formation of long-arm multipods. Furthermore, we tried to change the nature of reactants. In control experiments, when CdO was replaced by cadmium oleate, and/or Se was replaced by TOP-Se, multipod morphology can still be preserved. That is to say that adopted synthetic approach. Furthermore, experimental results demonstrated that the morphology of the obtained CdSe NCs was not sensitive to the experimental variables studied. We tried to extend this noninjection synthetic approach to the preparation of other II-VI group semiconductor NCs. Our primary results showed that this method is also successful in the preparation of CdS and CdTe and the demonstration results are available in Supporting Information. Extending exploration of this synthetic strategy is under further investigation.

CONCLUSIONS

In summary, gram-scale CdSe multipods were facilely prepared via a noninjection route in high yield with use of CdO and Se powder directly as reactants in paraffin reaction media. After deposition of ZnS around the CdSe multipod NCs, the PL QY of the obtained CdSe/ZnS can be up to 85%. Accordingly our reported preparation approach can satisfy the requirement of industrial production bearing the advantage of low-cost, reproducible, and scalable. Furthermore, this facile noninjection strategy provides a versatile route to large-scale preparation of other semiconductor NCs with multipod or other morphologies.

ASSOCIATED CONTENT

Supporting Information

Experimental details, TEM images under different experimental conditions, FFT of 2D lattice fringes, and results for preparation of CdS and CdTe. This material is available free of charge via the Internet at <http://pubs.acs.org>.

AUTHOR INFORMATION

Corresponding Author

*Fax: +86 21 6425 0281. E-mail: zhongxh@ecust.edu.cn.

ACKNOWLEDGMENTS

We thank the National Natural Science Foundation of China (No. 21175043), the Science and Technology Commission of Shanghai Municipality (11JC1403100), the Fundamental Research Funds for the Central Universities, and the Program for Professor of Special Appointment at Shanghai Institutions of Higher Learning for financial supports.

REFERENCES

- (1) Talapin, D. V.; Lee, J. S.; Kovalenko, M. V.; Shevchenko, E. V. *Chem. Rev.* **2010**, *110*, 389–458.
- (2) (a) Manna, L.; Milliron, D. J.; Meisel, A.; Scher, E. C.; Alivisatos, A. P. *Nat. Mater.* **2003**, *2*, 382–385. (b) Liu, H. T.; Alivisatos, A. P.

Nano Lett. **2004**, *4*, 2397–2401. (c) Gur, I.; Fromer, N. A.; Chen, C. P.; Kanaras, A. G.; Alivisatos, A. P. *Nano Lett.* **2007**, *7*, 409–414.

(3) (a) Mokari, T.; Rothenberg, E.; Popov, I.; Costi, R.; Banin, U. *Science* **2004**, *304*, 1787–1790. (b) Li, Y.; Zhong, H.; Li, R.; Zhou, Y.; Yang, C.; Li, Y. *Adv. Funct. Mater.* **2006**, *16*, 1705–1716. (c) Fang, L.; Park, J. Y.; Cui, Y.; Alivisatos, P.; Shcrier, J.; Lee, B.; Wang, L. W.; Salmeron, M. J. *Chem. Phys.* **2007**, *127*, 184704. (d) Nobile, C.; Ashby, P. D.; Schuck, P. J.; Fiore, A.; Mastria, R.; Cingolani, R.; Manna, L.; Krahn, R. *Small* **2008**, *4*, 2123–2126.

(4) (a) Sambur, J. B.; Novet, T.; Parkinson, B. A. *Science* **2010**, *330*, 63–66. (b) Borys, N. J.; Walter, M. J.; Huang, J.; Talapin, D. V.; Lupton, J. M. *Science* **2010**, *330*, 1371–1374.

(5) (a) Zhong, X.; Feng, Y.; Zhang, Y.; Lieberwirth, I.; Knoll, W. *Small* **2007**, *3*, 1194–1199. (b) Lazzarini, L.; Salviati, G.; Fabbri, F.; Zha, M.; Calestani, D.; Zappettini, A.; Sekiguchi, T.; Dierre, B. *ACS Nano* **2009**, *3*, 3158–3164.

(6) Cozzoli, P. D.; Manna, L.; Curri, M. L.; Kudera, S.; Giannini, C.; Striccoli, M.; Agostiano, A. *Chem. Mater.* **2005**, *17*, 1296–1306.

(7) (a) Jun, Y.; Jung, Y.; Cheon, J. J. *Am. Chem. Soc.* **2002**, *124*, 615–621. (b) Chen, M.; Xie, Y.; Lu, J.; Xiong, Y.; Zhang, S.; Qian, Y.; Liu, X. J. *Mater. Chem.* **2002**, *12*, 748–753. (c) Yong, K.; Sahoo, Y.; Swihart, M. T.; Prasad, P. N. *J. Phys. Chem. C* **2007**, *111*, 2447–2458. (d) Zhuang, Z.; Lu, X.; Peng, Q.; Li, Y. *J. Am. Chem. Soc.* **2010**, *132*, 1819–1821. (e) Govan, J. E.; Jan, E.; Querejeta, A.; Kotov, N. A.; Gunko, Y. K. *Chem. Commun.* **2010**, *46*, 6072–6074.

(8) (a) Donega, C. D.; Liljeroth, P.; Vanmaekelbergh, D. *Small* **2005**, *1*, 1152–1162. (b) Li, Y. C.; Zhong, H. Z.; Li, R.; Zhou, Y.; Yang, C. H.; Li, Y. F. *Adv. Funct. Mater.* **2006**, *16*, 1705–1716. (c) Kumar, S.; Nann, T. *Small* **2006**, *2*, 316–329. (d) Pang, Q.; Zhao, L.; Cai, Y.; Nguyen, D. P.; Regnault, N.; Wang, N.; Yang, S.; Ge, W.; Ferreira, R.; Bastard, G.; Wang, J. *Chem. Mater.* **2005**, *17*, 5263–5267. (e) Malkmus, S.; Kudera, S.; Manna, L.; Parak, W. J.; Braun, M. J. *Phys. Chem. B* **2006**, *110*, 17334–17338. (f) Li, Y.; Zhong, H.; Li, R.; Zhou, Y.; Yang, C.; Li, Y. *Adv. Funct. Mater.* **2006**, *16*, 1705–1716. (g) Cho, J. W.; Kim, H. S.; Kim, Y. J.; Jang, S. Y.; Park, J. *Chem. Mater.* **2008**, *20*, 5600–5609. (h) Nobile, C.; Ashby, P. D.; Schuck, P. J.; Fiore, A.; Mastria, R.; Cingolani, R.; Manna, L.; Krahn, R. *Small* **2008**, *4*, 2123–2126.

(9) (a) Manna, L.; Scher, E. C.; Alivisatos, A. P. *J. Am. Chem. Soc.* **2000**, *122*, 12700–12706. (b) Peng, Z. A.; Peng, X. *J. Am. Chem. Soc.* **2002**, *124*, 3343–3353. (c) Mohamed, M. B.; Tonti, D.; Salman, A. A.; Chergui, M. *ChemPhysChem* **2005**, *6*, 2505–2507. (d) Pang, Q.; Zhao, L.; Cai, Y.; Nguyen, D. P.; Regnault, N.; Wang, N.; Yang, S.; Ge, W.; Ferreira, R.; Bastard, G.; Wang, J. *Chem. Mater.* **2005**, *17*, 5263–5267. (e) Asokan, S.; Krueger, K. M.; Colvin, V. L.; Wong, M. S. *Small* **2007**, *3*, 1164–1169. (f) Huang, J.; Kovalenko, M. V.; Talapin, D. V. *J. Am. Chem. Soc.* **2010**, *132*, 15866–15868. (g) Ko, W. Y. L.; Bagaria, H. G.; Asokan, S.; Lina, K. J.; Wong, M. S. *J. Mater. Chem.* **2010**, *20*, 2474–2478.

(10) Jana, S.; Goswami, S.; Nandya, S.; Chattopadhyay, K. K. *J. Alloys Compd.* **2009**, *481*, 806–810.

(11) (a) Yong, K. T.; Sahoo, Y.; Choudhury, K. R.; Swihart, M. T.; Minter, J. R.; Prasad, P. N. *Nano Lett.* **2006**, *6*, 709–714. (b) Na, Y. J.; Kim, H. S.; Park, J. *J. Phys. Chem. C* **2008**, *112*, 11218–11226.

(12) Xie, R.; Kolb, U.; Basche, T. *Small* **2006**, *2*, 1454–1457.

(13) (a) Talapin, D. V.; Nelson, J. H.; Shevchenko, E. V.; Aloni, S.; Sadtler, B.; Alivisatos, A. P. *Nano Lett.* **2007**, *7*, 2951–2959. (b) Fiore, A.; Mastria, R.; Lupo, M. G.; Lanzani, G.; Giannini, C.; Carlino, E.; Morello, G.; De Giorgi, M.; Li, Y.; Cingolani, R.; Manna, L. *J. Am. Chem. Soc.* **2009**, *131*, 2274–2282. (c) Mahler, B.; Lequeux, N.; Dubertret, B. *J. Am. Chem. Soc.* **2010**, *132*, 953–959.

(14) Xia, X.; Liu, Z.; Du, G.; Li, Y.; Ma, M. *J. Phys. Chem. C* **2010**, *114*, 13414–13420.

(15) (a) Murray, C. B.; Norris, D. J.; Bawendi, M. G. *J. Am. Chem. Soc.* **1993**, *115*, 8706–8715. (b) Talapin, D.; Rogach, A. L.; Kornowski, A.; Haase, M.; Weller, H. *Nano Lett.* **2001**, *1*, 207–211. (c) Peng, Z. A.; Peng, X. *J. Am. Chem. Soc.* **2001**, *123*, 183–184. (d) Qu, L.; Peng, X. *J. Am. Chem. Soc.* **2002**, *124*, 2049–2055. (e) Donega, C. D. M.; Hickey, S. G.; Wuister, S. F.; Vanmaekelbergh,

D.; Meijerink, A. *J. Phys. Chem. B* **2003**, *107*, 489–496. (f) Deng, Z.; Cao, L.; Tang, F.; Zou, B. *J. Phys. Chem. C* **2005**, *109*, 16671–16675.

(g) Zhong, X.; Feng, Y.; Zhang, Y. *J. Phys. Chem. C* **2007**, *111*, 526–529. (h) Zlateva, G.; Zhelev, Z.; Bakalova, R.; Kanno, I. *Inorg. Chem.* **2007**, *46*, 6212–6214. (i) Liu, L.; Peng, Q.; Li, Y. *Inorg. Chem.* **2008**, *47*, 5022–5028. (j) Liu, L.; Zhuang, Z.; Xie, T.; Wang, Y.-G.; Li, J.; Peng, Q.; Li, Y. *J. Am. Chem. Soc.* **2009**, *131*, 16423–16429.

(16) (a) Zhong, X.; Han, M.; Dong, Z.; White, T.; Knoll, W. *J. Am. Chem. Soc.* **2003**, *125*, 8589–8594. (b) Zhong, X.; Feng, Y.; Knoll, W.; Han, M. *J. Am. Chem. Soc.* **2003**, *125*, 13559–13563.

(17) (a) Zhang, W.; Chen, G.; Wang, J.; Ye, B.; Zhong, X. *Inorg. Chem.* **2009**, *48*, 9723–9731. (b) Chen, G.; Zhang, W.; Zhong, X. *Front. Chem. CN.* **2010**, *5*, 214–220.

(18) (a) Li, J. J.; Guo, W.; Keay, J. C.; Mishima, T. D.; Johnson, M. B.; Peng, X. *J. Am. Chem. Soc.* **2003**, *125*, 12567–12575. (b) Xie, R.; Kolb, U.; Li, J.; Basche, T.; Mews, A. *J. Am. Chem. Soc.* **2005**, *127*, 7480–7488.